MOLECULAR AND CELLULAR BIOLOGY, July 1993, p. 4039–4048
0270-7306/93/074039-10$02.00/0

Vol. 13, No. 7

SKN1 and *KRE6* Define a Pair of Functional Homologs Encoding Putative Membrane Proteins Involved in β-Glucan Synthesis

TERRY ROEMER, SHAWN DELANEY, AND HOWARD BUSSEY*

Biology Department, McGill University, 1205 Dr. Penfield Avenue, Montreal, Quebec, Canada H3A 1B1

Received 18 February 1993/Returned for modification 25 March 1993/Accepted 19 April 1993

***KRE6* encodes a predicted type II membrane protein which, when disrupted, results in a slowly growing, killer toxin-resistant mutant possessing half the normal level of a structurally wild-type cell wall (1→6)-β-glucan (T. Roemer and H. Bussey, Proc. Natl. Acad. Sci. USA 88:11295–11299, 1991). The mutant phenotype and structure of the *KRE6* gene product, Kre6p, suggest that it may be a β-glucan synthase component, implying that (1→6)-β-glucan synthesis in *Saccharomyces cerevisiae* is functionally redundant. To examine this possibility, we screened a multicopy genomic library for suppression of both the slow-growth and killer resistance phenotypes of a *kre6* mutant and identified *SKN1*, which encodes a protein sharing 66% overall identity to Kre6p. *SKN1* suppresses *kre6* null alleles in a dose-dependent manner, though disruption of the *SKN1* locus has no effect on killer sensitivity, growth, or (1→6)-β-glucan levels. *skn1 kre6* double disruptants, however, showed a dramatic reduction in both (1→6)-β-glucan levels and growth rate compared with either single disruptant. Moreover, the residual (1→6)-β-glucan polymer in *skn1 kre6* double mutants is smaller in size and altered in structure. Since single disruptions of these genes lead to structurally wild-type (1→6)-β-glucan polymers, Kre6p and Skn1p appear to function independently, possibly in parallel, in (1→6)-β-glucan biosynthesis.**

Genetic redundancy permits specialization of cellular function and greater sophistication of regulatory control in cellular metabolism and growth. Gene families contribute to such redundancy and are an increasingly recurring theme even in eukaryotes such as *Saccharomyces cerevisiae* and *Schizosaccharomyces pombe*, which have small genomes. The genetic and biochemical tractability of *S. cerevisiae* has recently allowed the demonstration of partially redundant gene families involved in the synthesis of the polysaccharides chitin and glycogen (5, 6, 12, 13, 38, 41). Chitin synthesis requires three synthases which share substantial sequence homology and conserved topology. Their relative contributions to chitin synthesis in vivo, and to the deposition of chitin within the cell, vary widely. *CHS2* is required for laying down a normal primary septum, a disc-like structure composed largely of chitin that is deposited perpendicular to the bud neck to partition mother and daughter cells as budding nears completion (36). *CHS3* encodes the predominant in vivo chitin synthase, which makes 95% of the chitin deposited in the cell wall during vegetative growth (5, 36, 41). *CHS3* is also required postmeiotically, for synthesis of the chitin used to form the chitosan layer of the spore wall (3). *CHS1* is a third minor chitin synthase, postulated to have a repair function (6, 11).

Glycogen biosynthesis in yeast cells requires two isoforms of glycogen synthase, encoded by *GSY1* and *GSY2*, which share 80% identity at the protein level (12, 13). *GSY2* encodes the major glycogen synthase, as *gsy2* mutants show a 90% reduction in glycogen synthase activity, while *gsy1* mutants have a more modest 15% reduction. Strains possessing *gsy1 gsy2* double mutations lack detectable synthase activity. This redundancy provides flexibility in regulation; Gsy1p provides a minor constitutive glycogen synthase activity, while Gsy2p-specific glycogen synthase activity rises severalfold during stationary phase, concomitant with glycogen accumulation.

To what extent genetic redundancy occurs in genes involved in the synthesis of other polysaccharides is unclear. Redundancy in the synthetic components of (1→3)-β-glucan, the major yeast cell wall polysaccharide, has been suggested to explain the lack of biosynthetic mutants, as this situation would require mutations in more than one gene to completely block synthesis of the polymer (32). (1→3)-β-Glucan is thought to serve an essential role in conferring mechanical support against osmotic stress, and isolation of temperature-sensitive lysis mutants could directly identify genes involved in the synthesis of this polymer. Yet in both *S. cerevisiae* and *S. pombe*, such an approach has met with limited success. Lytic mutants have identified only putative components involved in the regulation of (1→3)-β-glucan synthesis, such as protein kinase C (22, 29, 31).

In studies on the biology of (1→6)-β-glucan, we have isolated a number of killer toxin-resistant, or *kre* mutants, with defects in cellular levels of this polymer (2, 4, 8, 27, 32), some of which suggest possible genetic redundancy. (1→6)-β-Glucan is an abundant cell surface polymer widely found among the fungi (15). In *S. cerevisiae*, this homopolymer of 140 to 200 glucose residues is composed largely of (1→6), with a substantial percentage of (1→6),(1→3) triply linked residues (2, 25). K1 killer toxin is a virus-encoded secreted protein which kills sensitive cells (7). The toxin binds to a cell surface receptor which contains a (1→6)-β-glucan component and subsequently forms lethal cation channels in the plasma membrane (19, 26, 44). Many of the *kre* mutants have reduced levels of (1→6)-β-glucan, and in the absence of a clear understanding of β-glucan synthesis in any eukaryote, these genes offer a genetic approach to the problem. A brief synopsis follows: *KRE5* encodes a putative soluble endoplasmic reticulum protein essential for (1→6)-β-glucan syn-

* Corresponding author.

TABLE 1. Yeast strains used in this study

Strain	Genotype	Source or reference
SEY6210	*MATα leu2-3,112 ura3-52 his3-Δ200 lys2-801 trp1-Δ901 suc2-Δ9*	S. D. Emr
TA405	*MATa/MATα his3/his3 leu2/leu2 can1/can1*	M. Whiteway
YDK5-1C	*MATa his3 leu2 can1*	27
TR92	*MATa kre6::HIS3 leu2-3,112 ura3-52 his3-Δ200 lys2-801 trp1-Δ901 suc2-Δ9*	32
TR98	*MATα kre6::HIS3 his3 leu2 can1*	32
TR144	*MATα kre6*::Tn*10 leu2-3,112 his3-Δ200 lys2-801 trp1-Δ901 suc2-Δ9*	32
TR145	*MATa kre6*::Tn*10 leu2-3,112 his3-Δ200 lys2-801 trp1-Δ901 suc2-Δ9*	32
TR160	*MATa/MATα SKN1/skn1::LEU2 his3/his3 leu2/leu2 can1/can1*	This work
TR166	*MATα skn1::LEU2 his3 leu2 can1*	This work; tetrad from TR160
TR167	*MATα skn1::LEU2 his3 leu2 can1*	This work; tetrad from TR160
TR168	*MATa SKN1 his3 leu2 can1*	This work; tetrad from TR160
TR169	*MATa SKN1 his3 leu2 can1*	This work; tetrad from TR160
TR165	*MATa/MATα SKN1/skn1::LEU2 leu2-3,112/leu2-3 ura3-52/ura3-52 his3-Δ200/his3-Δ200 lys2-801/lys2-801 trp1-Δ901/trp1-Δ901 suc2-Δ9/suc2-Δ9*	This work
TR178	*MATα skn1::LEU2 leu2-3,112 ura3-52 his3-Δ200 lys2-801 trp1-Δ901 suc2-Δ9*	This work; tetrad from TR165
TR179	*MATa skn1::LEU2 leu2-3,112 ura3-52 his3-Δ200 lys2-801 trp1-Δ901 suc2-Δ9*	This work; tetrad from TR165
TR180	*MATa SKN1 leu2-3,112 ura3-52 his3-Δ200 lys2-801 trp1-Δ901 suc2-Δ9*	This work; tetrad from TR165
TR181	*MATα SKN1 leu2-3,112 ura3-52 his3-Δ200 lys2-801 trp1-Δ901 suc2-Δ9*	This work; tetrad from TR165
TR69	*MATa/MATα KRE6/kre6::HIS3*	32
TR113	*KRE6 his3 leu2 can1*	This work; tetrad from TR69
TR114	*kre6::HIS3 his3 leu2 can1*	This work; tetrad from TR69
TR115	*KRE6 his3 leu2 can1*	This work; tetrad from TR69
TR116	*kre6::HIS3 his3 leu2 can1*	This work; tetrad from TR69
TR190	*MATa/MATα KRE6/kre6::HIS3 SKN1/skn1::LEU2 his3/his3 leu2/leu2 can1/can1*	This work
TR211	*kre6::HIS3 skn1::LEU2 his3 leu2 can1*	This work; segregant from TR190
TR212	*kre6::HIS3 skn1::LEU2 his3 leu2 can1*	This work; segregant from TR190
TR213	*kre6::HIS3 skn1::LEU2 his3 leu2 can1*	This work; segregant from TR190
TR214	*kre6::HIS3 skn1::LEU2 his3 leu2 can1*	This work; segregant from TR190
TR363	*MATa/MATα KRE6/kre6*::Tn*10 TEF1/tef1-Δ1324::URA3 ura3-52/ura3-52 leu2-3,112/leu2-3,112 HIS3/his3-Δ200 LYS2/lys2-801 trp1-Δ901/trp1-Δ1 SUC2/suc2-Δ9*	TR145 × MY2195
TR366	*MATa/MATα KRE6/kre6*::Tn*10 Ty1-48/Ty1-48::LEU2 KAR3/kar3-1*::pMR806 *RAD56/rad56-1 ARO7/aro7 ura3-52/ura3-52 leu2-3,112/leu2-3,112 HIS3/his3-Δ200 lys2/lys2-801 TRP1/trp1-Δ901 SUC2/suc2-Δ9*	TR144 × MY2254
MY2195	*MATα ura3-52 leu2-3,112 trp1-Δ1 tef1-Δ1324::URA3*	M. D. Rose
MY2254	*MATa ura3 leu2-3,112 lys2 aro7 rad56-1 Ty1-48::LEU2 kar3-1*::pMR806	
HAB792	*MATα skn1::LEU2 kre11::HIS3 ura3-52 his3-Δ200 leu2-3,112 trp1-Δ901 lys2-801*	4
HAB795	*MATa/MATα SKN1/skn1::LEU2 KRE11/kre11::HIS3 RSR1/rsr1::URA3 ADE3/ade3 LYS2/lys2-801 HIS3/his3-Δ200 ure3-52/ura3 leu2/leu2-3,112 trp1-Δ901/trp1*	4
Y355	*MATa rsr1::URA3 ade3 ura3 leu2 trp1*	A. Bender

thesis (27). *KRE6* encodes a probable type II membrane protein; in its absence, only half the amount of a wild-type (1→6)-β-glucan polymer is found (32). *KRE11* encodes a predicted cytoplasmic protein with a similar (1→6)-β-glucan null phenotype (4). *KRE1* is a serine/threonine-rich secretory pathway protein with a C-terminal hydrophobic tail. Null mutants of *KRE1* make a reduced level of the (1→6)-β-glucan which is distinct from wild type in being smaller and altered in structure (2). On the basis of these mutant phenotypes and their genetic interactions, a model of stepwise synthesis of (1→6)-β-glucan through the secretory pathway has been proposed (4, 8).

A pertinent feature of this model is a predicted genetic redundancy in the biosynthetic apparatus. Mutants harboring defects in either the *KRE6* or *KRE11* gene have only half the normal level of the (1→6)-β-glucan, and an explanation for these partial phenotypes is the presence of additional genes with partially overlapping function. We have tested for this possibility in the case of *KRE6*. We reasoned that if a functional homolog of *KRE6* were responsible for providing the remaining wild-type polymer in a *kre6* null background, then overproducing the homolog may increase synthesis of the (1→6)-β-glucan and suppress the *kre6* defect. Screening of a multicopy yeast library for the ability to restore growth and killer sensitivity to a *kre6* mutant has led to the identification of the *KRE6* homolog, *SKN1*.

MATERIALS AND METHODS

Yeast strains and methods. A *kre6::HIS3* null strain, TR92 (Table 1), was used for all screening and suppression analysis. Autodiploidized strains SEY6210 and TA405 were used for *skn1* disruptions. Yeast transformations were done by the lithium acetate method of Ito et al. (21), using 100 μg of sheared, denatured carrier DNA (35). Transformants were selected on synthetic complete medium (YNB) lacking uracil. Sensitivity to K1 killer toxin was scored by a seeded plate assay (9), using a modified medium consisting of minimal medium of Halvorson (16) with 6.7 g of YNB per liter 2.5 g of casein hydrolysate per liter, 0.0025% tryptophan, 1.5% Bacto Agar, 0.001% methylene blue, and 2% glucose. A sedimentation phenotype of *kre6* and *skn1* null strains was observed in YEPD buffered at pH 4.7 with Halvorson minimal medium (16) or YNB supplemented with 0.25% casein hydrolysate. Yeast DNA was isolated by the method of Hoffman and Winston (18).

***SKN1* isolation, plasmids, and constructions.** *SKN1* was isolated from a 2μm-based YEp24 yeast genomic library, by

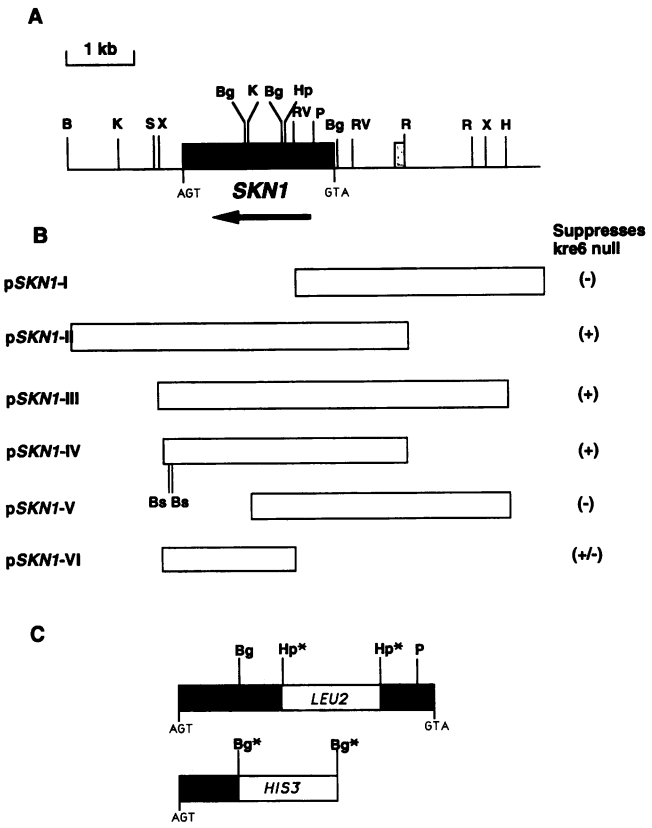

FIG. 1. (A) Restriction map of *SKN1*. The location of *SKN1* is indicated by the black box, and the direction of its transcription is shown by the arrow. A Ty element sequence is marked by the stippled box. Whether this element extends to the right of the *Eco*RI site (R) is unknown. Additional, unmapped *Hin*dIII sites (H) lie downstream of *SKN1* between *Sal*I (S) and *Bam*HI sites (B). Other restriction sites mapped are as follows: Bg, *Bgl*II; Hp, *Hpa*I; K, *Kpn*I; RV, *Eco*RV; and X, *Xba*I. (B) *SKN1* subclones and their ability (+) or inability (−) to suppress the *kre6* null phenotype in TR92. Two *Bsu*36I sites used in a C-terminal deletion in p*SKN1*-IV (see Materials and Methods) are designated Bs. (C) Summary of *SKN1* disruptions constructed. An asterisk marks the loss of the restriction site during subcloning.

selecting for Ura$^+$ transformants and screening for growth restoration and killer sensitivity in TR92, as described by Boone et al. (2). To identify *SKN1* within a 7-kb genomic fragment, the YEp24-*SKN1* isolate, 79-1, was restriction mapped (Fig. 1A), fragments were subcloned into YEp352 (Fig. 1B) and retransformed into TR92, and suppression was assessed. A 3.7-kb *SKN1* *Eco*RI-*Sal*I fragment with full *SKN1* suppression activity (p*SKN1*-IV) was subcloned into YCp50, a centromere-based vector for copy number suppression analysis. This fragment was also cloned in PBSKII (pPBSK-*SKN1*) for sequencing. A C-terminal truncation of *SKN1* was made by digesting two unique *Bsu*36I sites which lie within the last 174 bp of the *SKN1* open reading frame in p*SKN1*-IV (Fig. 1B), gel purifying the material to remove the 174-bp *Bsu*36I fragment, and religating the material. This plasmid, p*SKN1*-Bsu36I, lacks the last 48 codons of *SKN1* and contains 8 new codons before a TAA codon is reached.

Disruptions. A 3.7-kb *Sca*I-*Pvu*II *LEU2*-containing fragment was isolated from pRS305 and blunt-end ligated into the dephosphorylated *Hpa*I site of pPBSK-*SKN1* to construct the *skn1*::*LEU2* insertion-disruption construct, pPBSK-*skn1*::*LEU2*. *LEU2* is inserted 816 bp downstream of the ATG codon and 135 bp 5′ to the sequence encoding the transmembrane domain (TMD), thus presumably encoding a truncated Skn1p lacking a TMD sequence. pPBSK-*skn1*::*LEU2* was *Sal*I-*Xho*I digested, and total digested material was transformed into two isogenic diploids, TA405 and SEY6210. Leu$^+$ transformants were sporulated, and tetrad analysis revealed a 2:2 segregation of leucine prototrophy. Gene disruptions were confirmed by both Southern and Northern (RNA) blot analyses (24).

In addition, a deletion-disruption construct of *SKN1* (pPBSK-*skn1*::*HIS3*) was created. Digestion of pPBSK-*SKN1* with *Bgl*II, which removes two fragments totaling 1.3 kb of open reading frame, was followed by alkaline phosphatase treatment and gel purification of this vector for ligation with a 1.7-kb *HIS3*-containing *Bam*HI fragment. pPBSK-*skn1*::*HIS3* was digested with *Eco*RI and *Sal*I and transformed into diploid strains TA405 and SEY6210. Haploid *skn1*::*HIS3* null strains were isolated following tetrad dissection, and their authenticity was checked by Southern analysis.

Mapping. *SKN1* was mapped to chromosome VII by the use of a 1.2-kb *Kpn*I-*Xba*I *SKN1* random-primed probe (Pharmacia) to hybridize to a gel wafer (Clontech) of separated *S. cerevisiae* chromosomes (data not shown). More precise physical mapping of both *SKN1* and *KRE6* was achieved following hybridization of the above-described *SKN1* probe and a 2.0-kb *Hin*dIII-*Nde*I *KRE6* probe to grids containing a λ phage library of yeast genomic inserts (provided by L. Riles). *SKN1* maps to λ clones 3545 and 4734, which overlap by 10 kb, and *KRE6* maps to λ clone 6672. Genetic mapping of *kre6* involved crossing strains TR145 and TR144 to strains MY2195 and MY2254, respectively. The resulting diploids, TR363 and TR366, were sporulated, and tetrads were analyzed. Yeast strains MY2195 and MY2254 were from M. Rose. To genetically map *skn1*, diploid HAB795 (4) was sporulated and subjected to tetrad analysis. Strain HAB795 was made by crossing Y355, obtained from A. Bender, to HAB792.

DNA sequencing. Subclones of *SKN1* were made in the PBSKII vector and transformed into *Escherichia coli* UT580, and single-stranded DNA was prepared by using M13K07 helper phage (42). Sequencing was done by the dideoxy-chain termination method of Sanger et al. (34), using the Sequenase kit from United States Biochemicals. Universal, reverse, or a variety of synthesized oligonucleotides complementary to specific regions of the *SKN1* DNA sequence were used as primers to yield the complete sequence of both strands of a 3.7-kb *Eco*RI-*Sal*I region.

β-Glucan analysis. Alkali-insoluble glucan was isolated from stationary-phase cultures grown in YEPD (Tables 3 and 5) and YNB (Fig. 2). (1→6)-β-Glucan was prepared after digestion of alkali-insoluble glucan with the (1→3)-β-glucanase preparation zymolyase (ICN Pharmaceuticals, Inc., Irvine, Calif.) (2). Total alkali-insoluble (1→3)- and (1→6)-β-glucan was determined as the sum of the carbohydrate content of both the zymolyase-insoluble pellet and the solubilized supernatant before dialysis. Analysis of the carbohydrate retained after dialysis gave the amount of alkali-insoluble (1→6)-β-glucan. Carbohydrate was measured as hexose (1). Large-scale preparations of (1→6)-β-glucan were made for ^{13}C nuclear magnetic resonance analysis as described by Boone et al. (2). Gel filtration chromatography to estimate the average size of *skn1* and *kre6* single-null and *skn1* *kre6* double-null (1→6)-β-glucans was performed by using a Sepharose CL-6B column as described previously

Plasmid	(1-6)-β-Glucan (μg/mg Dry Wt.)	(1-3)-β-Glucan (μg/mg Dry Wt.)	Seeded Plate Zone Size
YCp50	20.0 ± 4.6	139.0 ± 25.6	
YEp352	21.7 ± 3.4	137.1 ± 14.3	
YCp50-*SKN1*	31.5 ± 4.5	137.1 ± 10.2	
YEp352-*SKN1*	37.6 ± 3.3	147.3 ± 13.2	
YCp50-*KRE6*	42.4 ± 4.9	157.8 ± 11.2	

FIG. 2. Effect of *SKN1* copy number on suppression of in vivo *kre6* null β-glucan defects. Plasmids transformed into *kre6* null TR92 are indicated on the left. YCp50 is a centromere-based low-copy-number plasmid; YEp352 is a multicopy, 2μm-based plasmid. Killer toxin sensitivity as measured by the seeded plate assay is shown on the right. Also shown are in vivo (1→6)- and (1→3)-β-glucan levels measured as described in Materials and Methods. Error represents 1 standard deviation.

(2), and the hexose content of eluted fractions was determined (1).

(1→3)-β-Glucan synthase assay. Cell extracts were prepared from early-log-phase cells grown in YEPD, harvested, and homogenized by vortexing with glass beads in buffer A (50 mM Tris-HCl [pH 7.5], 0.5 mM EDTA, 33% [vol/vol] glycerol). Protein concentrations were estimated by using the Bio-Rad protein assay. Particulate (1→3)-β-glucan synthase activity was assayed as outlined by Cabib and Kang (10), with the omission of bovine serum albumin and EDTA. Assays were carried out at 30°C for 60 min in 5 mM UDP-glucose 0.5 mM GTPγ S, 25 mM KF, 1 mM β-mercaptoethanol, and 3.0 ml of UDP-[^{14}C]glucose (355 mCi/mmol; Amersham, Oakville, Ontario, Canada) plus yeast protein extract in buffer A. Specific activities are expressed as nanomoles of glucose incorporated per milligram of protein per hour. Estimation of UDP-[^{14}C]glucose incorporated into trichloroacetic acid-insoluble material was measured as described by Szaniszlo et al. (40).

RESULTS

Cloning of *SKN1* by multicopy suppression of a *kre6* mutant. To isolate multicopy suppressors to the killer resistance and slow-growth phenotypes of *kre6*, a *kre6* null strain was transformed with a YEp24-based yeast genomic library containing the *URA3* selectable marker and screened for killer sensitivity and wild-type growth. After screening of approximately 20,000 Ura$^+$ transformants, 11 plasmids were isolated and classified into two sets on the basis of their plasmid-dependent phenotypes and restriction maps. The first set, isolated six times, was *KRE6*. The second set, distinct from *KRE6*, was represented by five independently isolated genomic fragments of two sizes with nearly 6 kb of overlapping sequence, and the responsible gene was named *SKN1*, for suppressor of a *kre6* null mutation. A restriction map of a 7-kb *SKN1* fragment was determined, and a variety of subclones were generated in the YEp352 vector (Fig. 1A and B). *SKN1* was subcloned to a 3.7-kb *Eco*RI-*Sal*I fragment (p*SKN1*-IV; Fig. 1B) which completely suppressed the growth defect of a *kre6* null strain and conferred a toxin sensitivity approaching that of the wild type (Fig. 2). One smaller subclone (p*SKN1*-VI) partially suppressed the slow growth of a *kre6* null strain but did not correct for killer sensitivity (Fig. 1B and 3).

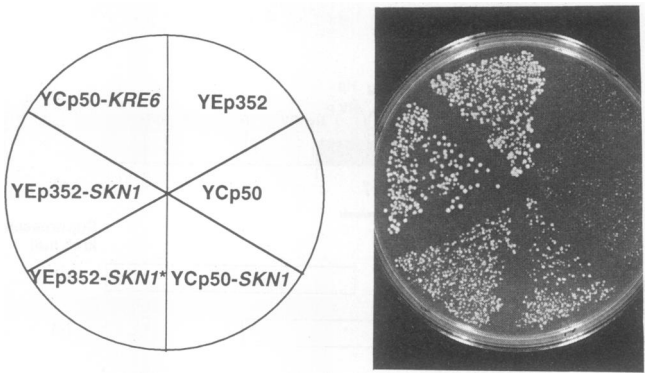

FIG. 3. Relative growth defect suppression of *kre6* null TR92 as a function of *SKN1* copy number. YEp352-*SKN1* and YEp352-*SKN1** are subclones p*SKN1*-IV and p*SKN1*-VI, respectively (see Fig. 1B). YCp50-*KRE6* is plasmid p504 as described by Roemer and Bussey (32).

Mapping of *SKN1* and *KRE6*. *SKN1* and *KRE6* were physically mapped to specific locations on chromosomes VII and XVI, respectively, following chromosome blotting and assignment to ordered lambda clones containing the yeast genome (see Materials and Methods). *SKN1* was localized to the right arm of chromosome VII, near *RSR1*, while *KRE6* hybridized to DNA situated at the end of the right arm of chromosome XVI, adjacent to *KAR3*. Genetic mapping of *skn1* and *kre6* was consistent with their physical map locations (Table 2). *skn1* maps 11 centimorgans from *rsr1*, with the data in Table 2 indicating the gene order as *CEN7 skn1 rsr1 kre11 ade3*. The *kre6* locus was mapped to a position 2 centimorgans centromere distal to *kar3* in the order *CEN16 tef1* Ty1-48 *kar3 kre6* (Table 2). DNA sequence determined 3′ to *KRE6* identified *GPH1*, a gene encoding glycogen phosphorylase and previously assigned to either chromosome XVI or chromosome XIII (20). A composite restriction map of *KRE6* and *GPH1* indicates their relative locations (Fig. 4).

Sequence of *SKN1*. Sequencing the 3.7-kb fragment from p*SKN1*-IV revealed an open reading frame of 2,313 nucleotides encoding a protein of 86 kDa with striking homology to Kre6p (Fig. 5). Like Kre6p, Skn1p is predicted to encode a putative type II membrane protein (17, 30) containing substantial N-terminal cytoplasmic (288 amino acid residues) and lumenal (452 amino acid residues) domains separated by a TMD of 31 hydrophobic residues. The two predicted

TABLE 2. Genetic mapping of the *SKN1* and *KRE6* loci

Locus	Interval	Tetrad type			Map distance (centimorgans)
		PD	NPD	TT	
SKN1	*skn1-rsr1*	80	0	22	11
	skn1-kre11	37	4	80	43
	skn1-ade3	20	5	78	58
	kre11-rsr1	35	3	49	39
	kre11-ade3	91	0	11	5
KRE6	*kre6-tef1*	30	6	58	50
	kre6-Ty1-48	64	0	26	14
	kre6-kar3	91	0	3	2
	kar3-Ty1-48	65	0	23	13

proteins have an overall identity in excess of 66%, with the lumenal domains showing 86% identity. Homology continues over a stretch of 125 residues N proximal to the TMD but decreases substantially toward the N termini of the proteins. Six potential asparagine-linked glycosylation sites lie within the proposed lumenal domain of Skn1p. An asparagine-rich tract at residues 127 to 136 as well as a serine/threonine-rich stretch between residues 330 and 340 of Skn1p are both absent from Kre6p. No additional homologs of *SKN1* were found with sequences in the GenBank data base.

At the DNA level, identity between the lumenal domain-encoding regions of *KRE6* and *SKN1* is 76%, implying no recent divergence in these genes. Intriguingly, a 120-nucleotide stretch of a Ty delta sequence (analogous to a retroviral long terminal repeat) lies 1 kb 5′ to the *SKN1* start codon. It is not known whether this is one end of a complete Ty element or is a solo delta sequence. No clear homology exists between the *KRE6* and *SKN1* promoter sequences. Northern analysis indicates that both *KRE6* and *SKN1* transcripts are present in YEPD-grown cells and are 2.8 kb in length. In addition, transcript levels of *SKN1* do not vary in a *kre6* null mutant (data not shown).

***SKN1* is a dosage-dependent suppressor of a *kre6* null mutation.** To test for copy number effect on suppression, *SKN1* was introduced into the centromeric and multicopy plasmids YCp50 and YEp352, and suppression of a *kre6* null mutation was examined. Multicopy *SKN1* was shown to restore growth, killer sensitivity, and (1→6)-β-glucan levels in *kre6* null strains to levels close to those found in the wild type (Fig. 2 and 3). In contrast, *SKN1* expression from the centromeric plasmid conferred a more modest suppression, judged by growth and (1→6)-β-glucan levels. *SKN1* is thus a functional homolog of *KRE6*, capable of suppressing a *kre6* disruption in a dosage-dependent manner.

Although no comprehensive deletion/mutagenesis analysis of *SKN1* has been undertaken, preliminary subcloning experiments hint at the relative importance of the cytoplasmic and lumenal domains of the *SKN1* product in suppressing a *kre6* null mutation. The multicopy *SKN1* subclone p*SKN1*-VI (Fig. 1B), constructed by using an internal *Eco*RV site deleting the first 186 amino-terminal residues of cytoplasmic domain-predicted sequence, can partially suppress a *kre6* null growth defect despite having lost all 5′ promoter sequence and presumably relying on a cryptic plasmid-based promoter (Fig. 3). In contrast, p*SKN1*-Bsu36I, containing a deletion of the C-terminal 48 amino acids (Fig. 1B), failed to suppress a *kre6* null mutation (data not shown).

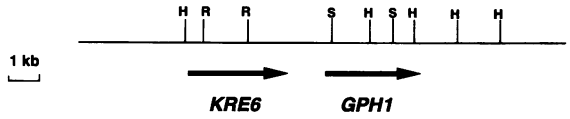

FIG. 4. Physical map of *KRE6* and *GPH1* on the right arm of chromosome XVI. Arrows represent the direction of transcription for the open reading frames. Restriction sites are symbolized as in Fig. 1A.

Disruption of *SKN1*. A Rothstein (33) one-step gene replacement of *SKN1* was carried out by using a *LEU2* marker (see Materials and Methods). Tetrad analysis of spore progeny derived from both TA405 and SEY6210 *skn1*::*LEU2* heterozygotes indicated that haploid *skn1*::*LEU2* cells grew at rates comparable to those of the wild type and were killer toxin sensitive (Fig. 6). In contrast to *kre6* null mutants, analysis of alkali-insoluble glucan levels from *skn1* null haploids showed no significant reduction in the level of (1→6)-β-glucan (Table 3). ^{13}C nuclear magnetic resonance analysis and column chromatography of the alkali-insoluble (1→6)-β-glucan from *skn1* nulls indicated the polymer to be wild type in both structure and size (data not shown). The *skn1* lesion appeared to have no effect on homologous matings, on sporulation of homozygotes, or on spore germination. However, *skn1* null mutants were found to sediment faster than isogenic wild-type strains in liquid medium. This phenotype was neither enhanced by 2 mM $CaCl_2$ nor inhibited by 20 mM EDTA.

A concern, based on both the phenotype and the fact that an N-terminal truncation of Skn1p (p*SKN1*-VI) was partially active, was that the *skn1*::*LEU2* insertion-disruption generated a leaky allele. To exclude this possibility, an additional disruption which deleted 60% of the gene, including sequence encoding the TMD, was made (see Materials and Methods and Fig. 1C). Like *skn1*::*LEU2* mutants, *skn1*::*HIS3* mutant strains grew normally, with normal in vivo levels of β-glucan, and were sensitive to killer toxin.

We previously reported a partial reduction in both in vivo (1→3)-β-glucan levels and in vitro (1→3)-β-glucan synthase activity in *kre6* null strains (32). On the basis of in vitro and in vivo defects in the synthesis of the (1→3)-β-glucan polymer, we proposed *KRE6* involvement in the synthesis of this polysaccharide as well as of (1→6)-β-glucan. A prediction from these results is that a related defect might be seen in a *skn1* mutant, and the *kre6* defect should be amplified in a *skn1 kre6* double mutant. Examination of (1→3)-β-glucan synthase activity in *skn1* null extracts shows a minor in vitro defect (Table 4); however, no in vivo reduction in (1→3)-β-glucan polymer levels was found (Table 3).

Phenotypes of *skn1 kre6* double mutants. To test whether the *kre6*::*HIS3 skn1*::*LEU2* double disruption possessed a more severe phenotype than that conferred by disruption of these genes singly, strains harboring a *kre6* or *skn1* mutation were crossed in both the SEY6210 and TA405 backgrounds, and diploids were sporulated for tetrad analysis. Tetrad analysis of *kre6 skn1* double heterozygotes in strain SEY6210 demonstrated that the double-null mutation was lethal in this genetic background. A total of 19 tetrads were dissected to yield 13 tetratypes (TT), 3 parental ditypes (PD), and 3 nonparental ditypes (NPD), of which only 1 of the 19 predicted doubly disrupted spores underwent a single cell division. Double disruptants were viable in strain TA405, as 23 tetrads from two independent diploids yielded 16 TT, 4 PD, and 3 NPD, as judged by His^+ and Leu^+ prototrophy. Double *kre6 skn1* null strains grew extremely slowly relative to *kre6* or *skn1* single-null strains (Fig. 6A and B). To assess glucan levels in these *kre6 skn1* mutant strains, spontaneous

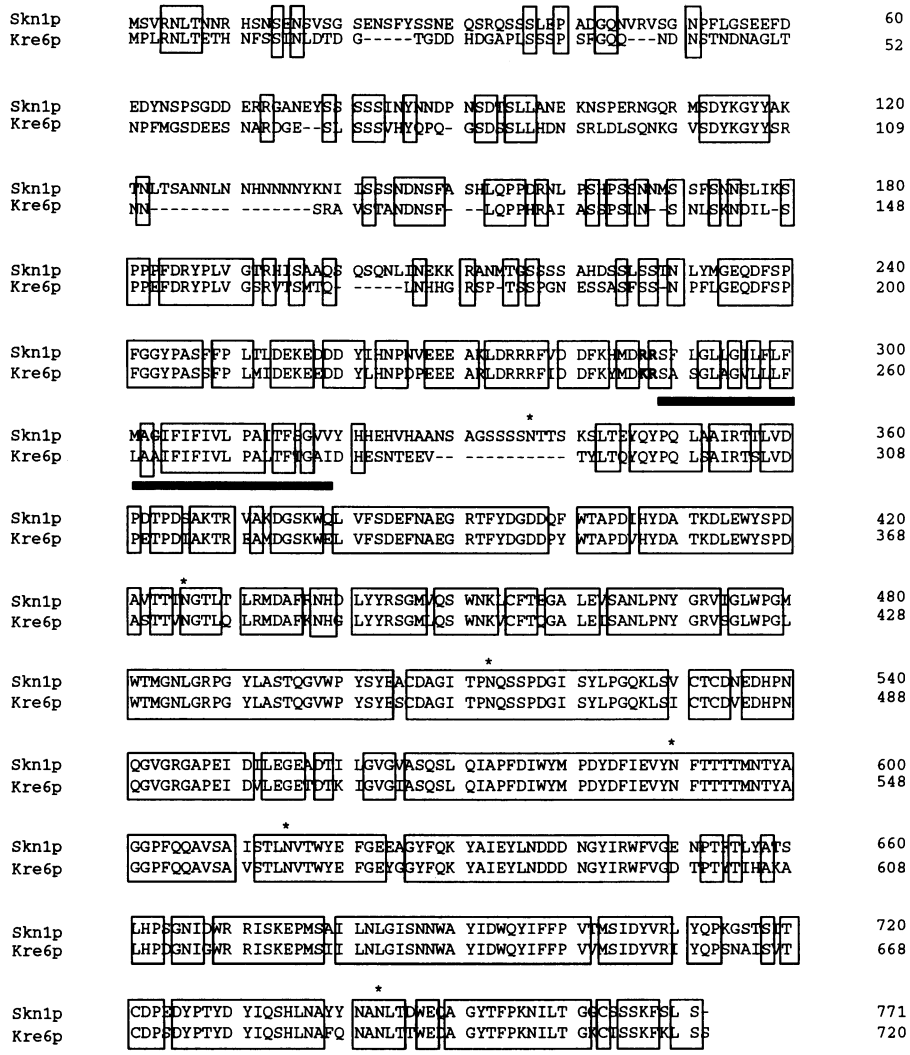

FIG. 5. Sequences and comparison of the *SKN1*- and *KRE6*-encoded proteins Skn1p and Kre6p. The proteins are shown in the single-letter amino acid code and are aligned to show identities, which are boxed. The protein names are shown at the left; the amino acid residue numbers are shown at the right. Gaps introduced to improve alignment are indicated by dashes. Several features of the proteins are indicated; the TMDs are underlined, and pairs of basic residues amino terminal to the TMDs are identified in boldface letters. On the basis of a predicted type II topology, cytoplasmic domains lie amino terminal to their respective TMDs, and lumenal/periplasmic domains are carboxy terminal. Possible asparagine-linked glycosylation sites on the carboxy-terminal lumenal/periplasmic domains are marked by asterisks.

suppressors which weakly alleviated the growth impairment were isolated. Seeded plate zone size comparisons between *kre6 skn1* double-null strains and *kre6* single-null strains demonstrated an enhanced killer resistance phenotype; the small, fuzzy zone seen with TA405-based *kre6* null strains was completely absent in *kre6 skn1* double-null strains (Fig. 6B). Analysis of alkali-insoluble glucan levels from four independently suppressed *kre6 skn1* double mutants indicated a reduction in (1→6)-β-glucan of 70 to 80% relative to the wild type (Table 5). This reduction is exaggerated over levels for *kre6* mutants, which possess an approximately 50% decrease, or the wild-type levels found in *skn1* strains. Of the residual carbohydrate material in the (1→6)-β-glucan fraction that was isolated from *kre6 skn1* mutants, approximately 70% could be enzymatically digested with the glycogen-degrading enzymes α-amylase and pullulanase. ^{13}C nuclear magnetic resonance analysis indicated that (1→6)-linked glucose residues remained, although these represented only a small proportion of the material (data not shown). Given this finding, *kre6 skn1* double mutants are estimated to have no more than 10% of the wild-type level of (1→6)-β-glucan. In addition to the *skn1*::*LEU2* allele, a *skn1*::*HIS3 kre6*::*HIS3* double mutation was made in TA405. This strain was viable, albeit extremely slowly growing, and was indistinguishable from the TA405-based *skn1*::*LEU2 kre6*::*HIS3* double disruptant.

Table 5 indicates that the suppressed *skn1 kre6* double mutants had normal or slightly elevated levels of (1→3)-β-glucan. To explore a possible (1→3)-β-glucan defect further, we assayed for (1→3)-β-glucan synthase activity in vitro (Table 4). The level of the synthase was reduced relative to the wild type, but this reduction was not amplified over the lower levels found in either the *kre6* or *skn1* disruption singly. Because the issue of the possible involvement of *kre6*

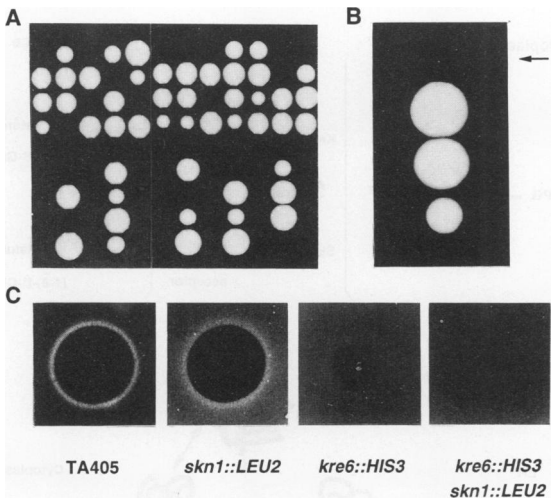

FIG. 6. Phenotypes of *skn1*, *kre6*, and *skn1 kre6* double null strains. (A) Spore progeny from a *skn1::LEU2 kre6::HIS3* double heterozygous TA405 diploid (TR190) dissected onto YEPD. Large colonies are identified as wild-type or *skn1* null strains, small colonies are *kre6* null strains, and microcolonies or the absence of a colony indicates *skn1 kre6* double null strains, inferred by scoring prototrophic markers. (B) Enlargement of a dissected tetratype tetrad in panel A to reveal a *skn1 kre6* double-null microcolony (arrow). (C) Killer resistance phenotypes of the genotypes identified.

and *skn1* in (1→3)-β-glucan synthesis is important, we have reexamined the (1→3)-β-glucan polymer levels in *kre6* null strains but have been unable to reproducibly detect significant in vivo reduction, the values in Table 5 being typical.

Genetic interaction between *kre6* and *kre11* null mutations. Genetic interaction between mutants provides a framework for examining possible relationships between the cytoplasmic and secretory components required for the synthesis of (1→6)-β-glucan. Brown et al. (4) have demonstrated a genetic interaction between *kre6* and *kre11*, as strains harboring both *kre11-1* and *kre6::HIS3* alleles were shown to be lethal in a SEY6210 background. To extend this observation, we examined *kre11::HIS3 kre6*::Tn*10* double-null mutations in SEY6210 and found them to be lethal. Nineteen tetrads from two independent diploids displayed an ascus type of 13 TT, 2 PD, and 4 NPD, from which all predicted *kre11::HIS3 kre6*::Tn*10* double-null spores died after two to three cell divisions.

To test for possible symmetry in the genetic interaction of *KRE11* with both *KRE6* and its functional homolog *SKN1*, a *kre11::HIS3 skn1::LEU2* double mutant was made in SEY6210. These double-null mutants appeared identical to *kre11::HIS3* single mutants on the basis of growth and killer resistance.

TABLE 3. Levels of alkali-insoluble β-glucans in *SKN1* and *skn1* null mutants

Yeast strain	Allele at *SKN1* locus	Concn (μg/mg [dry wt])[a]	
		(1→6)-β-Glucan	(1→3) + (1→6)-β-Glucan
TR166	*skn1::LEU2*	23.2 ± 2.1	113.9 ± 8.9
TR167	*skn1::LEU2*	26.9 ± 3.4	112.1 ± 25.8
TR168	*SKN1*	26.9 ± 2.0	108.8 ± 8.3
TR169	*SKN1*	25.5 ± 3.1	112.4 ± 4.8
TR178	*skn1::LEU2*	29.3 ± 2.6	132.7 ± 4.7
TR179	*skn1::LEU2*	32.3 ± 2.6	126.8 ± 4.9
TR180	*SKN1*	31.9 ± 1.6	125.0 ± 5.1
TR181	*SKN1*	33.7 ± 2.0	119.9 ± 6.8

[a] Measured from spore progeny of dissected tetrads derived from autodiploidized strains TA405 and SEY6210 made heterozygous for the *skn1::LEU2* allele. Error represents 1 standard deviation.

TABLE 4. (1→3)-β-Glucan synthase activity in various *skn1* and *kre6* deletion mutants

Strain	Allele at *SKN1* or *KRE6* locus	(1→3)-β-Glucan synthase sp act (nmol/mg/h)[a]
TR166	*skn1::LEU2*	85.1 ± 13.1
TR167	*skn1::LEU2*	95.5 ± 1.7
TR168	*SKN1*	149.2 ± 4.8
TR169	*SKN1*	136.2 ± 0.9
TR113	*kre6::HIS3*	53.0 ± 1.5
TR114	*KRE6*	111.9 ± 0.7
TR115	*kre6::HIS3*	33.0 ± 2.1
TR116	*KRE6*	145.0 ± 1.6
TR211	*skn1::LEU2 kre6::HIS3*	90.7 ± 0.4
TR214	*skn1::LEU2 kre6::HIS3*	74.4 ± 2.6

[a] Error represents 1 standard deviation.

DISCUSSION

A screen based on multicopy suppression of *kre6* mutant phenotypes has led to the identification of *SKN1*. *SKN1* encodes a protein sharing 66% identity, and a type II membrane protein topology, with Kre6p. *SKN1* suppressed *kre6* null alleles in a dose-dependent manner, although disruption of the *SKN1* locus had no effect on killer sensitivity, on growth, or on (1→6)-β-glucan level or structure. A rapid sedimentation phenotype was evident in *skn1* null strains. This sedimentation phenotype, which was also found in *kre6* mutants, suggests some alteration at the cell surface and may be of value in industrial fermentations. The *skn1 kre6* double mutants show a major reduction in both (1→6)-β-glucan levels and growth rate, and the mutations are lethal in the SEY6210 background. Moreover, the (1→6)-

TABLE 5. Levels of alkali-insoluble β-glucans in four independent *kre6/skn1* double disruptants harboring second-site suppressors

Yeast strain	Genotype	Concn (μg/mg [dry wt])[a]	
		(1→6)-β-Glucan	(1→3) + (1→6)-β-Glucan
TR211	*kre6::HIS3 skn1::LEU2*	7.0 ± 1.2	105.4 ± 3.5
TR212	*kre6::HIS3 skn1::LEU2*	7.9 ± 1.9	161.5 ± 3.8
TR213	*kre6::HIS3 skn1::LEU2*	9.0 ± 2.0	175.0 ± 5.1
TR214	*kre6::HIS3 skn1::LEU2*	8.1 ± 1.8	154.2 ± 2.7
TR98	*kre6::HIS3 SKN1*	21.1 ± 3.5	92.2 ± 6.1
YDK5-1C	*KRE6 SKN1*	29.5 ± 3.5	119.2 ± 4.0

[a] β-Glucan levels from four spontaneously suppressed *skn1/kre6* double nulls (TR211 to TR214) were examined as described in Materials and Methods. Second-site suppressors were isolated by successive streaking of double-disruptant spore progeny onto YEPD plates to constant colony size. Strains TR98 and YDK5-1C show β-glucan levels in TA405-based *kre6::HIS3* and wild-type haploids, respectively. Error represents standard deviation.

β-glucan polymer in *skn1 kre6* double mutants is smaller in size and altered in structure. *SKN1* and *KRE6* constitute a new gene family of putative type II membrane proteins in *S. cerevisiae* that are implicated in (1→6)-β-glucan synthesis.

KRE6 and *SKN1* are required for the majority of the cellular alkali-insoluble (1→6)-β-glucan and appear to function independently, since single disruptions lead to wild-type (1→6)-β-glucan polymers of variable abundance. *KRE6* would appear to be the more active member of the pair, as its absence leads to a strong growth phenotype, killer resistance, and a 50% reduction in the polymer. *SKN1* seems to participate in a less significant way, as deletion of the gene has little effect or at least can be largely compensated for in the presence of *KRE6*. However, *SKN1* appears to be relied on more heavily in the absence of *KRE6*, as the *kre6 skn1* double-mutant phenotype is far more severe than either a *kre6* or *skn1* defect alone. The *SKN1* gene can suppress a *kre6* null mutation by overexpression from a multicopy plasmid. *SKN1* does not appear to compensate transcriptionally for the absence of *KRE6*, as Northern analysis demonstrates that expression of the genomic copy of *SKN1* is not substantially up-regulated in a *kre6* null strain. The basis of the relative importance of Kre6p and Skn1p in glucan synthesis is unknown but could be based on their abundance, stability, regulation, or functional activity. The substantial divergence in protein sequence between the N-terminal cytoplasmic domains of the two proteins could, for example, allow for their differential interaction with cytoplasmic regulatory proteins.

The possible role of *KRE6* and *SKN1* in (1→3)-β-glucan synthesis remains unclear; both genes when disrupted lead to modest reductions in in vitro (1→3)-β-glucan synthase levels, and overproduction of *KRE6* leads to an increase in the level of this activity. However, no synergistic drop in the level of (1→3)-β-glucan synthase activity is seen in the double mutant. While the *kre6 skn1* double mutant clearly demonstrates the need for the *KRE6 SKN1* gene pair for in vivo (1→6)-β-glucan synthesis, no such in vivo reduction is seen with (1→3)-β-glucan. Either the *KRE6* and *SKN1* genes are not directly involved in (1→3)-β-glucan synthesis or there are other redundant genes involved in the process. Interestingly, elevated levels of (1→3)-β-glucan are often detected in suppressed *kre6 skn1* double-null and *kre5-1* strains (2), suggesting that severe (1→6)-β-glucan defects may be compensated for in some way by additional (1→3)-β-glucan.

A model depicting a possible pathway for (1→6)-β-glucan biosynthesis is shown in Fig. 7. *KRE5* is placed at the earliest step in the pathway, on the basis of the absence of detectable (1→6)-β-glucan when this gene is disrupted and its putative endoplasmic reticulum localization (27). By analogy with eukaryotic glycogen biosynthesis (23, 39), the small residual amount of (1→6)-β-glucan in a *kre6 skn1* double mutant may be associated with a *KRE5*-dependent primer, which is elaborated in the presence of *KRE6* and *SKN1*. Disruptions of *KRE6* or *SKN1* singly do not appear to affect the structure of the polymer, which implies that these two gene products act within parallel branches of a (1→6)-β-glucan pathway and are candidates for membrane-associated subunits of related and partially redundant synthases. The Kre6p and Skn1p membrane proteins may effect coupling between cytoplasmic and secretory components of the (1→6)-β-glucan synthetic apparatus. Evidence supporting this notion rests with the genetic findings that *kre11 kre6* double-null mutations are lethal (4) and that *kre5-1 kre6-1* strains possess an exaggerated reduction in (1→6)-β-glucan

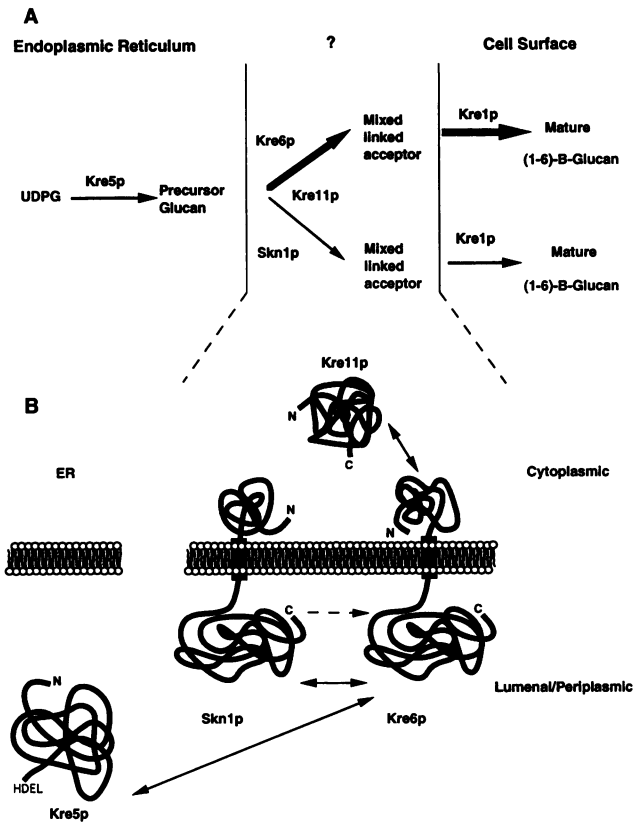

FIG. 7. (A) Schematic outline of a possible (1→6)-β-glucan biosynthetic pathway. Arrows represent points in a stepwise synthesis of the polymer; their thickness represents a relative flux based on phenotypes of the *kre6* and *skn1* single mutants. UDP-glucose (UDPG), although not formally shown to be the substrate, is suggested from (1→3)-β-glucan biosynthetic data to be so. Two different intermediate (1→6)-β-glucan polymers are described as a precursor/primer and a mixed linked acceptor, judged from analysis of the (1→6)-β-glucan polymer remaining in various null backgrounds as described in Discussion. The proposed cellular locations of these gene products are listed at the top; the question mark symbolizes undefined location. (B) Genetic interactions between gene products involved in (1→6)-β-glucan synthesis. The dashed arrow represents multicopy suppression of the null mutation of the gene to which the arrow points. Solid double arrows represent genetic interactions based on more severe phenotypes of double mutants. Cytoplasmic and lumenal/periplasmic compartments are labeled. ER, endoplasmic reticulum.

levels compared with single mutants (27). Such genetic interactions should be interpreted cautiously, but as Kre11p and Skn1p are required for (1→6)-β-glucan synthesis in the absence of *KRE6*, these two proteins might interact directly in a complex. *KRE1*, the most distal gene identified, is involved in the elaboration of an intermediate polymer to complete the synthesis of (1→6)-β-glucan (2). This model is based on genetic evidence supported by in vivo glucan phenotypes but lacks the biochemical evidence necessary to show that these gene products are directly involved in (1→6)-β-glucan synthesis. Formally, we may have identified genes that directly or indirectly affect any step in (1→6)-β-glucan synthesis, assembly, maintenance, or degradation.

Identifying the cellular location and possible physical interactions of the *KRE* and *SKN* gene products becomes an important task in substantiating any model. For example, do

Kre6p and Skn1p reside within the secretory pathway, or are they localized at the cell surface? On the basis of current knowledge of the cellular localization of biosynthetic enzymes making other cell wall polysaccharides, either outcome might be expected. Biochemical evidence from studies on enriched plasma membrane fractions suggests that the majority of (1→3)-β-glucan synthase activity in *S. cerevisiae* is localized at the cell surface (37). A plasma membrane location has also been suggested for cellulose and glucan synthases in the oomycete *Saprolegnia monoica* (14). However, in plants, biochemical and immunocytochemical data demonstrate that cell wall polysaccharides such as xyloglucans, arabinogalactans, and pectins are synthesized in the Golgi complex and secreted to the cell surface (28, 43).

ACKNOWLEDGMENTS

We thank Jeff Brown, Bo Jiang, and Nathalie Fortin for advice and discussions, Jeff Brown and Zuzana Kossaczka for help with gene mapping, and Diane Oki for manuscript preparation. We also thank Linda Riles for providing lambda grids and interpreting hybridization results, and we thank Alan Bender and Mark Rose for sending mapping strains.

This work was supported by Operating and Strategic grants from the National Sciences and Engineering Council of Canada. T.R. is an NSERC postgraduate fellow.

REFERENCES

1. **Badin, J., C. Jackson, and M. Schubert.** 1953. Improved method for determination of plasma polysaccharides with tryptophan. Proc. Soc. Exp. Biol. Med. **84:**228–291.
2. **Boone, C., S. S. Sommer, A. Hensel, and H. Bussey.** 1990. Yeast *KRE* genes provide evidence for a pathway of cell wall β-glucan assembly. J. Cell Biol. **110:**1833–1843.
3. **Briza, P., M. Breitenbach, A. Ellinger, and J. Segall.** 1990. Isolation of two developmentally regulated genes involved in spore wall maturation in *Saccharomyces cerevisiae*. Genes Dev. **4:**1775–1789.
4. **Brown, J. L., Z. Kossaczka, B. Jiang, and H. Bussey.** 1993. A mutational analysis of killer toxin resistance in *S. cerevisiae* identifies new genes involved in cell wall (1→6)-β-glucan synthesis. Genetics **133:**837–849.
5. **Bulawa, C. E.** 1992. *CSD2*, *CSD3*, and *CSD4*, genes required for chitin synthase in *Saccharomyces cerevisiae*: the *CSD2* gene product is related to chitin synthases and to developmentally regulated proteins in *Rhizobium* species and *Xenopus laevis*. Mol. Cell. Biol. **12:**1764–1776.
6. **Bulawa, C. E., M. Slater, E. Cabib, J. Au-Young, A. Sburlati, W. L. Adair, Jr., and P. W. Robbins.** 1986. The *S. cerevisiae* structural gene for chitin synthase is not required for chitin synthesis *in vivo*. Cell **46:**213–225.
7. **Bussey, H.** 1991. K1 killer toxin, a pore-forming protein from yeast. Mol. Microbiol. **5:**2339–2343.
8. **Bussey, H., C. Boone, J. Brown, K. Hill, T. Roemer, and A.-M. Sdicu.** 1992. (1-6)-β-Glucan biosynthesis: potential targets for antifungal drugs, p. 20–31. *In* P. Fernandes (ed.), New approaches for antifungal drugs. Birkhauser, Boston.
9. **Bussey, H., W. Sacks, D. Galley, and D. Saville.** 1982. Yeast killer mutations affecting toxin secretion and activity and toxin immunity function. Mol. Cell. Biol. **2:**346–354.
10. **Cabib, E., and M. S. Kang.** 1987. Fungal 1,3-β-glucan synthase. Methods Enzymol. **138:**637–642.
11. **Cabib, E., A. Sburlati, B. Bowers, and S. J. Silverman.** 1989. Chitin synthase 1, an auxiliary enzyme for chitin synthase in *Saccharomyces cerevisiae*. J. Cell Biol. **108:**1665–1672.
12. **Farkas, I., T. A. Hardy, A. A. DePaoli-Roach, and P. J. Roach.** 1990. Isolation of the *GSY1* gene encoding yeast glycogen synthase and evidence for the existence of a second gene. J. Biol. Chem. **265:**20879–20886.
13. **Farkas, I., T. A. Hardy, M. G. Goebl, and P. J. Roach.** 1991. Two glycogen synthase isoforms in *Saccharomyces cerevisiae* are coded by distinct genes that are differentially controlled. J. Biol. Chem. **266:**15602–15607.
14. **Fevre, M., V. Girard, and P. Nodet.** 1990. Cellulose and β-glucan synthesis in *Saprolegnia*, p. 97–107. *In* P. J. Kuhn, A. P. J. Trinci, M. J. Jang, M. W. Goosey, and L. G. Copping (ed.), Biochemistry of cell walls and membranes in fungi. Springer-Verlag, Berlin.
15. **Fleet, G. H., and H. J. Phaff.** 1981. Fungal glucans—structure and metabolism, p. 416–440. *In* W. Tanner and F. A. Loewus (ed.), Encyclopedia of plant physiology new series, vol. 13B. Plant carbohydrates II. Springer-Verlag, Berlin.
16. **Halvorson, H. O.** 1958. Studies on protein and nucleic acid turnover in growing cultures of yeast. Biochim. Biophys. Acta **27:**267–276.
17. **Harthann, E., T. A. Rapoport, and H. F. Lodish.** 1989. Predicting the orientation of eukaryotic membrane-spanning domains. Proc. Natl. Acad. Sci. USA **86:**5786–5790.
18. **Hoffman, C., and F. Winston.** 1987. A ten-minute DNA preparation from yeast efficiently releases autonomous plasmids for transformation of *Escherichia coli*. Gene **57:**267–272.
19. **Hutchins, K., and H. Bussey.** 1983. Cell wall receptor for yeast killer toxin: involvement of (1→6)-β-glucan. J. Bacteriol. **154:** 161–169.
20. **Hwang, P. K., S. Tugendreich, and R. J. Fletterick.** 1989. Molecular analysis of *GPH1*, the gene encoding glycogen phosphorylase in *Saccharomyces cerevisiae*. Mol. Cell. Biol. **9:**1659–1666.
21. **Ito, H., M. Fukuda, M. Murata, and A. Kimura.** 1983. Transformation of intact yeast cells with alkali cations. J. Bacteriol. **153:**63–68.
22. **Levin, D. E., and E. Bartlett-Heubusch.** 1992. Mutants in the *S. cerevisiae PKC1* gene display a cell cycle-specific osmotic stability defect. J. Cell Biol. **116:**1221–1229.
23. **Lomako, J., M. Lomako, and W. J. Whelan.** 1990. The nature of the primer for glycogen synthesis in muscle. FEBS Lett. **268:** 8–12.
24. **Maniatis, T., E. F. Fritsch, and J. Sambrook.** 1989. Molecular cloning: a laboratory manual, 2nd ed. Cold Spring Harbor Laboratory, Cold Spring Harbor, N.Y.
25. **Manners, D. J., A. J. Masson, and J. C. Patterson.** 1973. The structure of a β-(1-6)-D-glucan from yeast cell walls. Biochem. J. **135:**31–36.
26. **Martinac, B., H. Zhu, A. Kubalski, X. Zhou, M. Culbertson, H. Bussey, and C. Kung.** 1991. Yeast killer toxin forms ion channels in sensitive yeast spheroplasts and in artificial liposomes. Proc. Natl. Acad. Sci. USA **87:**6228–6239.
27. **Meaden, P., K. Hill, J. Wagner, D. Slipetz, S. S. Sommer, and H. Bussey.** 1990. The yeast *KRE5* gene encodes a probable endoplasmic reticulum protein required for (1→6)-β-glucan synthase and normal cell growth. Mol. Cell. Biol. **10:**3013–3019.
28. **Moore, P. J., and L. A. Staehelin.** 1988. Immunogold localization of the cell-wall matrix polysaccharides rhamnogalacturonan I and xyloglucan during cell expansion and cytokinesis in *Trifolium pratense* L.; implication for secretory pathways. Planta **174:**433–445.
29. **Paravicini, G., M. Cooper, L. Friedli, D. J. Smith, J.-L. Carpentier, L. S. Klig, and M. A. Payton.** 1992. The osmotic integrity of the yeast cell requires a functional *PKC1* gene product. Mol. Cell. Biol. **12:**4896–4905.
30. **Parks, G. D., and R. A. Lamb.** 1991. Topology of eukaryote type II membrane proteins: importance of N-terminal positively charged residues flanking the hydrophobic domain. Cell **64:**777–787.
31. **Ribas, J. C., M. Diaz, A. Duran, and P. Perez.** 1991. Isolation and characterization of *Schizosaccharomyces pombe* mutants defective in cell wall (1-3)-β-D-Glucan. J. Bacteriol. **173:**3456–3462.
32. **Roemer, T., and H. Bussey.** 1991. Yeast β-glucan synthase: *KRE6* encodes a predicted type II membrane protein required for glucan synthesis *in vivo* and for glucan synthase activity *in vitro*. Proc. Natl. Acad. Sci. USA **88:**11295–11299.
33. **Rothstein, R. J.** 1983. One step gene-disruption in yeast. Methods Enzymol. **101:**202–211.
34. **Sanger, F., S. Nicklen, and A. R. Coulson.** 1977. DNA sequenc-

ing with chain-terminating inhibitors. Proc. Natl. Acad. Sci. USA **74**:5463–5467.
35. **Schiestl, R. H., and R. D. Gietz.** 1989. High efficiency transformation of intact yeast cells using single stranded nucleic acids as a carrier. Curr. Genet. **16**:339–346.
36. **Shaw, J. A., P. C. Mol, B. Bowers, S. J. Silverman, M. H. Valdivieso, A. Duran, and E. Cabib.** 1991. The function of chitin synthases 2 and 3 in the *Saccharomyces cerevisiae* cell cycle. J. Cell Biol. **114**:111–123.
37. **Shematek, E. M., J. A. Braatz, and E. Cabib.** 1980. Biosynthesis of the yeast cell wall. 1. Preparation and properties of β(1-3) glucan synthase. J. Biol. Chem. **255**:888–894.
38. **Silverman, S. J.** 1989. Similar and different domains of chitin synthases 1 and 2 of *S. cerevisiae*. Yeast **5**:459–467.
39. **Smythe, C., C. Villar-Palasi, and P. Cohen.** 1989. Structural and functional studies on rabbit liver glycogenin. Eur. J. Biochem. **183**:205–209.
40. **Szaniszlo, P. J., M. S. Kang, and E. Cabib.** 1985. Stimulation of β(1→3)glucan synthetase of various fungi by nucleoside triphosphates: generalized regulatory mechanism for cell wall biosynthesis. J. Bacteriol. **161**:1188–1194.
41. **Valdivieso, M. H., P. C. Mol, J. A. Shaw, E. Cabib, and A. Duran.** 1991. Cloning of *CAL1*, a gene required for activity of chitin synthase 3 in *Saccharomyces cerevisiae*. J. Cell Biol. **114**:101–109.
42. **Vernet, T., D. Dignard, and D. Y. Thomas.** 1987. A family of yeast expression vectors containing the phage f1 intergenic region. Gene **52**:225–233.
43. **Zhang, G. F., and L. A. Staehelin.** 1992. Functional compartmentalization of the Golgi apparatus of plant cells. Plant Physiol. **99**:1070–1083.
44. **Zhu, H., and H. Bussey.** 1991. Mutational analysis of the functional domains of yeast K1 killer toxin. Mol. Cell. Biol. **11**:175–181.